

Accepted Manuscript

Structure-activity relationships in a new class of non-substrate-like covalent inhibitors of the bacterial glycosyltransferase LgtC

Yong Xu, Jon Cuccui, Carmen Denman, Tripty Maharjan, Brendan W. Wren, Gerd K. Wagner

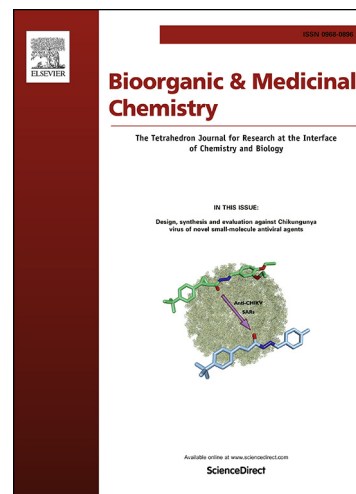
PII: S0968-0896(18)30135-4
DOI: <https://doi.org/10.1016/j.bmc.2018.03.006>
Reference: BMC 14244

To appear in: *Bioorganic & Medicinal Chemistry*

Received Date: 23 January 2018
Revised Date: 3 March 2018
Accepted Date: 4 March 2018

Please cite this article as: Xu, Y., Cuccui, J., Denman, C., Maharjan, T., Wren, B.W., Wagner, G.K., Structure-activity relationships in a new class of non-substrate-like covalent inhibitors of the bacterial glycosyltransferase LgtC, *Bioorganic & Medicinal Chemistry* (2018), doi: <https://doi.org/10.1016/j.bmc.2018.03.006>

This is a PDF file of an unedited manuscript that has been accepted for publication. As a service to our customers we are providing this early version of the manuscript. The manuscript will undergo copyediting, typesetting, and review of the resulting proof before it is published in its final form. Please note that during the production process errors may be discovered which could affect the content, and all legal disclaimers that apply to the journal pertain.



Structure-activity relationships in a new class of non-substrate-like covalent inhibitors of the bacterial glycosyltransferase LgtC

Yong Xu [1], Jon Cuccui [2], Carmen Denman [2], Tripty Maharjan [2], Brendan W. Wren [2] & Gerd K. Wagner [1]*

[1] King's College London, Department of Chemistry, Faculty of Natural & Mathematical Sciences, Britannia House, 7 Trinity Street, London, SE1 1DB, UK. Phone: +44 (0)20 7848 1926; e-mail: gerd.wagner@kcl.ac.uk

[2] Faculty of Infectious and Tropical Diseases, London School of Hygiene & Tropical Medicine

*Corresponding author

1 March 2018

Keywords: glycosyltransferase, covalent inhibitor, structure-activity relationship, bacterial virulence, serum resistance

Abstract

Lipooligosaccharide (LOS) structures in the outer core of Gram-negative mucosal pathogens such as *Neisseria meningitidis* and *Haemophilus influenzae* contain characteristic glycoepitopes that contribute significantly to bacterial virulence. An important example is the digalactoside epitope generated by the retaining α -1,4-galactosyltransferase LgtC. These digalactosides camouflage the pathogen from the host immune system and increase its serum resistance. Small molecular inhibitors of LgtC are therefore sought after as chemical tools to study bacterial virulence, and as potential candidates for anti-virulence drug discovery. We have recently discovered a new class of non-substrate-like inhibitors of LgtC. The new inhibitors act via a covalent mode of action, targeting a non-catalytic cysteine residue in the LgtC active site. Here, we describe, for the first time, structure-activity relationships for this new class of glycosyltransferase inhibitors. We have carried out a detailed analysis of the inhibition kinetics to establish the relative contribution of the non-covalent binding and the covalent inactivation steps for overall inhibitory activity. Selected inhibitors were also evaluated against a serum-resistant strain of *Haemophilus influenzae*, but did not enhance the killing effect of human serum.

1. Introduction

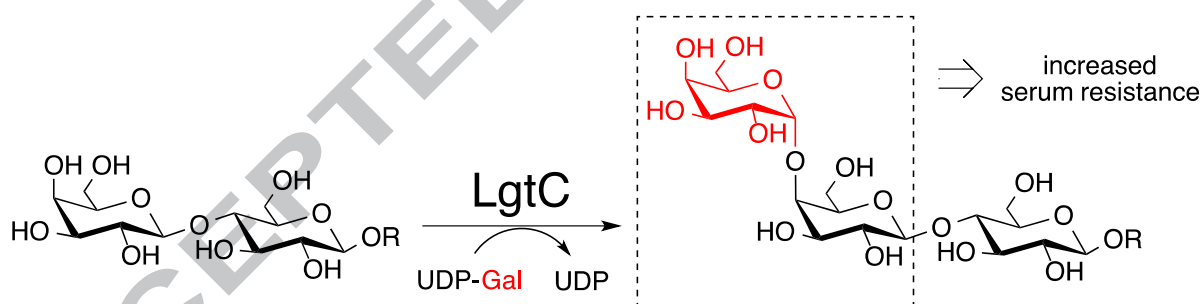
Glycoconjugates such as glycolipids and glycoproteins play a critical role for the virulence and viability of many bacterial pathogens [1]. The biosynthetic machinery required for bacterial glycoconjugate synthesis therefore offers a rich source of potential targets for the development of novel anti-bacterial or anti-virulence agents. A central role for bacterial glycoconjugate biosynthesis is played by glycosyltransferases (GTs), a family of enzymes that catalyse the transfer of a sugar from a glycosyl donor to a requisite acceptor [2]. It has been estimated that for most organisms, 1-3% of their genes encode GTs and other carbohydrate-active enzymes [3]. From the 1.6 Mb genome of *Campylobacter jejuni* NCTC 11168, for example, approximately 45 GTs have been predicted [4]. Individual bacterial GTs such as the *N*-acetylglucosamine transferase MurG, a key enzyme for peptidoglycan biosynthesis, have been identified as promising targets for the discovery of novel antibiotics [5].

Another important bacterial GT is the retaining α -1,4-galactosyltransferase LgtC [6], which catalyses the transfer of a D-galactose moiety from a UDP-D-galactose (UDP-Gal) donor to lactose-containing acceptors in the lipooligosaccharide (LOS) envelope of Gram-negative pathogens such as *Neisseria* and *Haemophilus* (Fig. 1). LgtC is a member of family GT-8 in the CAZy database of carbohydrate-active enzymes [7], and is highly conserved across different *Neisseria*, *Haemophilus* and *Pasteurella* species. The resulting digalactoside epitopes confer resistance to pre-existing antibody and complement-mediated lysis [8] and have been associated with increased virulence in an *in-vivo* model of *Haemophilus influenzae* infection [9]. The expression of LgtC has also been linked directly with the high-level serum resistance of *H. influenzae* R2866 [10]. Small molecular inhibitors of LgtC are therefore of

considerable interest as chemical tools for microbiological investigation and as potential lead compounds for anti-virulence drug discovery [11].

Previously reported LgtC inhibitors are mainly substrate-like molecules derived from the UDP-Gal donor [6,12]. Due to the presence of the charged diphosphate fragment and their potentially limited stability, such donor analogues are not suitable for applications with bacterial cultures or cells. We have recently discovered a novel class of non-substrate-like LgtC inhibitors based on a pyrazol-3-one scaffold (Fig. 2) [13]. These inhibitors behave as substrate mimics and react covalently, at their Michael acceptor system, with a non-catalytic cysteine in the LgtC active site [13]. Due to their uncharged, drug-like structure and straightforward synthesis, these pyrazol-3-ones are attractive for applications in chemical biology and drug discovery.

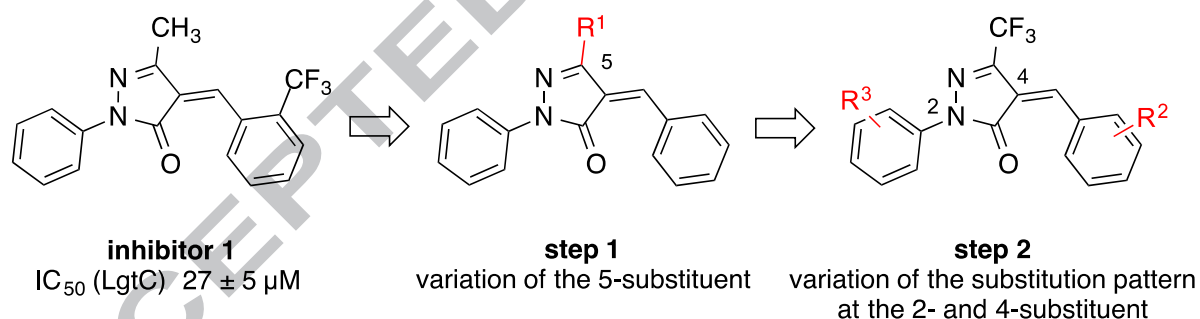
Fig. 1 The LgtC reaction



In the present study, we have systematically explored structural modifications around the pyrazol-3-one scaffold. Starting from prototype inhibitor **1** [13], we first designed and synthesised analogues with various substituents at the 5-position of the pyrazol-3-one scaffold (Fig. 2). We investigated a range of 5-substituents with different steric and electronic properties, in order to probe their effect on the reactivity of the Michael acceptor system. Following the identification of a 5-CF₃ substituent as advantageous, further structural optimisation was carried out on the 2-

and 4-position. To understand the relative contribution of the non-covalent binding step and the covalent inactivation step to the overall inhibition of LgtC, we carried out detailed covalent inhibition kinetics with selected derivatives. Determination of their inhibition constants K_i and inactivation rates k_{inact} and correlation of these parameters with IC_{50} values allowed us, for the first time, to establish SAR in this series. We also tested selected pyrazol-3-ones against *H. influenzae* strain R2866, both in growth inhibition and serum survival assays. Unfortunately, these inhibitors had no effect on serum resistance, and only a minimal effect on bacterial growth. Although these pyrazol-3-ones therefore have probably limited potential as drug candidates, our strategy and results provide a strong foundation for the rational design of alternative covalent inhibitor chemotypes for this enzyme as well as related bacterial GTs.

Fig. 2 Design strategy for pyrazol-3-one derivatives investigated in this study

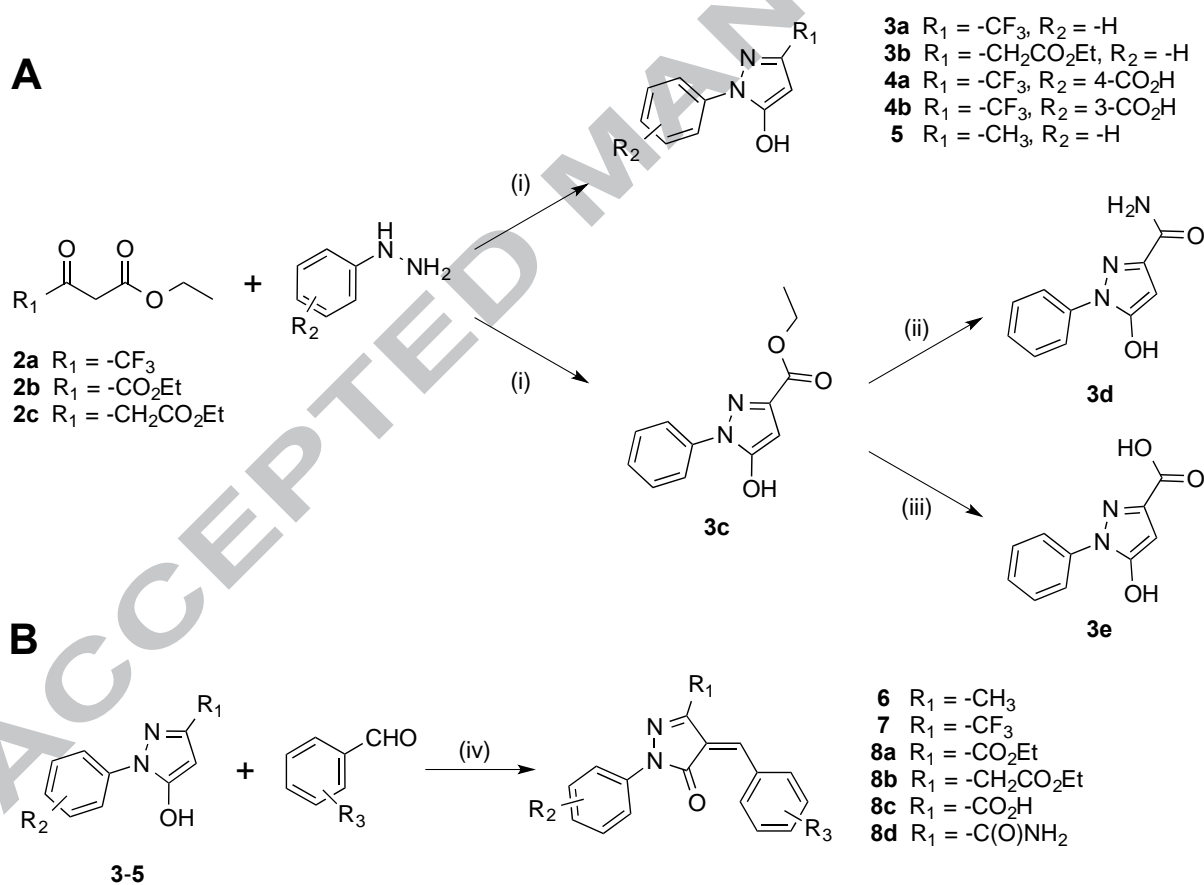


2. Results and discussion

2.1 Chemistry

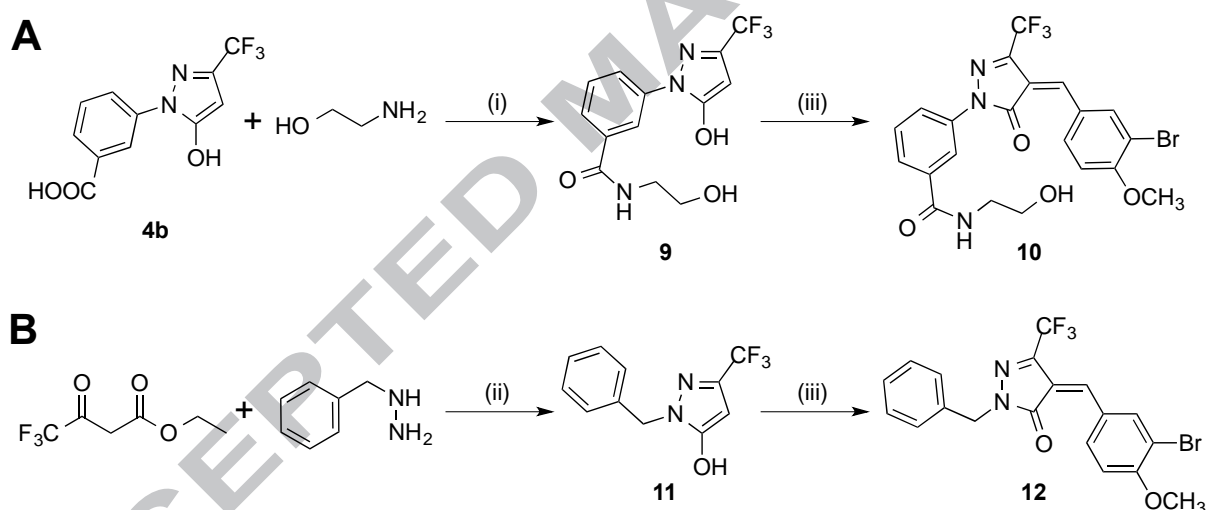
To obtain the target molecules, one of the key steps was the synthesis of intermediates with different substituents in the 5-position of the pyrazol-3-one scaffold (Scheme 1A). Six intermediates (**3a-3c**, **4a-b**, and **5**) were obtained by condensation reactions of commercially available aryl hydrazines and β -ketoesters

2a-c in acetic acid at 120 °C. The condensation products were obtained in 41-75% yield after purification by column chromatography. **3c** was then converted to other cyclised intermediates by different synthetic routes. **3c** was heated at reflux in 28% aqueous ammonia for 12 h to generate the amide derivative **3d**, while a hydrolysis reaction with **3c** afforded carboxylic acid derivative **3e**. With intermediates **3**, **4**, and **5** in hand, the benzylidene-substituted pyrazol-3-one products **6-8** were obtained by condensation with the respective aldehyde in moderate to good yield under microwave conditions (Scheme 1B).



Scheme 1. Synthesis of pyrazol-3-one derivatives **6-8**. *Reagents and conditions:* (i) AcOH, 110 °C, overnight, 41-75%; (ii) aq. NH₃ (28%), reflux, 38%; (iii) aq. NaOH (1 N), EtOH, rt, 91%; (iv) aldehyde, 160 °C, microwave, 15 mins, 15-80%. For substituents R₂ and R₃ see Tables 1-3.

Compounds **10** and **12** were prepared as shown in Scheme 2. The carboxylic acid intermediate **4b**, was reacted with 2-aminoethan-1-ol in the presence of diisopropylethylamine (DIEA) and 2-(1*H*-benzotriazol-1-yl)-1,1,3,3-tetramethyluronium hexafluorophosphate (HBTU) in DMF to afford amide **9**. (Scheme 2A). For the synthesis of intermediate **11**, ethyl 3-oxobutanoate was heated to reflux with benzylhydrazine in glacial acetic acid (Scheme 2B). The target compounds **10** and **12** were obtained from **9** and **11**, respectively, via condensation reaction with 3-bromo-4-methoxybenzaldehyde under the microwave conditions described above.



Scheme 2. Synthesis of pyrazol-3-one derivatives **10** and **12**. *Reagents and conditions:* (i) HBTU, DIEA, DMF, rt, 75%; (ii) AcOH, 110 °C, overnight, 17%; (iii) 3-bromo-4-methoxybenzaldehyde, 160 °C, microwave, 15 mins, 9% (**10**) or 28% (**12**).

The 1D NMR spectra of all benzylidene-substituted pyrazol-3-ones showed the presence of only a single geometric isomer (ESI). Consistently, the peak for the H-1 and/or H-6 proton at the benzylidene ring appeared distinctly downfield (>8.5 ppm). This downfield shift is caused by the deshielding effect of the carbonyl group on these protons in the (Z) isomer, and is therefore diagnostic for the (Z) configuration

of the double bond [14]. Further evidence for the (Z) configuration was obtained from a NOESY experiment with 5-methyl pyrazol-3-one **6** (ESI), which showed a NOE correlation between the protons of the 5-CH₃ group (δ 2.3 ppm) and the CH at the exocyclic double bond (δ 7.75). While a similar NOESY analysis is not applicable in the 5-CF₃ series, due to the absence of protons from position 5, the (Z) configuration of **6** is in keeping with the configuration observed in the crystal structure of a structurally related 5-CF₃ pyrazol-3-one [15].

2.2 Biochemical evaluation of inhibitors

2.2.1 Inhibition of LgtC

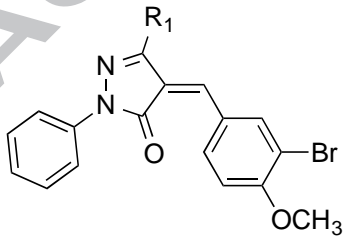
To assess the inhibitory activity of the pyrazolone derivatives, we used a colorimetric biochemical assay previously reported by our group [16]. In this enzyme-coupled assay, calf intestinal phosphatase (CIP) is used to selectively and quantitatively release inorganic phosphate (P_i) from UDP, the secondary product of the LgtC reaction, followed by quantification of P_i with Malachite Green. Because of the covalent mode of action previously observed in this inhibitor series [13], we pre-incubated the enzyme with inhibitor prior to starting the enzymatic reaction.

First, we assessed the potency of pyrazol-3-one derivatives with different substituents at the 5-position, but identical substituents at positions 2 and 4 (Table 1). Inhibitory activity was determined at two different concentrations of inhibitor (25 μ M and 50 μ M), and with 30 mins pre-incubation time. Under these conditions, the 5-CF₃-substituted derivative **7b** displayed the strongest inhibitory activity, with about 84% inhibition at 50 μ M. Practically all derivatives with an electron-withdrawing 5-substituent were more active than the electron-donating 5-methyl congener **6**, which showed only about half the level of inhibition of **7b**. These results suggested that

electron-withdrawing 5-substituents are advantageous for LgtC inhibition, possibly by increasing the reactivity of the Michael acceptor system. However, caution has to be applied when analysing the behaviour of covalent inhibitors, as their overall activity is determined not only by the reactivity of their electrophilic warhead, but also by their binding affinity at the target [17]. Variations in potency within this series of 5-substituted pyrazol-3-ones may therefore result not only from differences in Michael acceptor reactivity, but also from different non-covalent binding affinities. The decreased activity of compounds with bulky electron-withdrawing 5-substituents (**8c**, **8d**), for example, may be due to suboptimal non-covalent binding outweighing the increased reactivity of the Michael acceptor.

To better understand the interplay between covalent inactivation and non-covalent binding for overall inhibitory activity of these pyrazol-3-ones, we next investigated how different substituents on the 2-phenyl and 4-benzylidene moieties affect inhibitory activity in a series of analogues with the same 5-substituent. Based on initial SAR trends, we selected 5-CF₃ derivative **7b** as the starting point for this set of modifications (Table 2).

Table 1 Pyrazol-3-ones with different 5-substituents, and their inhibitory activity against LgtC.



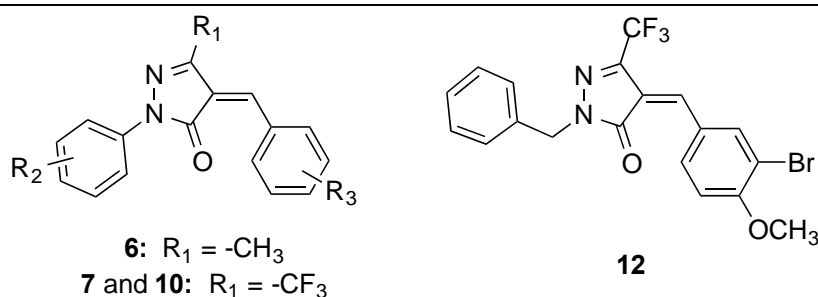
Cmpd	R ₁	inhibition (%) ^a	
		at 50 μM	at 25 μM
6	-CH ₃	43 ± 2	33 ± 0.1
7b	-CF ₃	84 ± 3	80 ± 4
8a	-CO ₂ Et	66 ± 3	61 ± 3

8b	-CH ₂ CO ₂ Et	67 ± 4	32 ± 5
8c	-CO ₂ H	58 ± 1	35 ± 1
8d	-C(O)NH ₂	39 ± 6	31 ± 6

^aLgtC was pre-incubated with inhibitor (25 μM or 50 μM) or DMSO, UDP-Gal (28 μM), MnCl₂ (5 mM), CIP (10 U/mL), CEL (1 mg/mL), and Triton (0.01%) for 30 mins at 30 °C in 13 mM HEPES buffer (pH 7.0). Lactose (2 mM) was added, and the reactions were incubated for 20 mins at 30 °C. Each compound was tested in triplicate; results are presented as average ± SD.

Derivative **7c** with an unsubstituted 4-benzylidene moiety showed approximately 10-fold weaker inhibition than reference inhibitor **7b**. Analogues of **7b** in which the 3-Br, 4-OCH₃ substitution pattern was replaced with a 3-OBn (**7a**) or 4-Cl (**7d**) group displayed a similar drop in potency. Introduction of a bulky group at the *ortho*-position of the 4-benzylidene ring (**7e**) completely abolished inhibitory activity, which suggested that sterically demanding substituents in this position are not tolerated by the enzyme. In contrast, compounds with different modifications at the 3- or 4-position of the 2-phenyl ring (**7f**, **7g**, and **10**) maintained similar inhibitory activity as the parent **7b**. These general SAR trends are consistent with previous results from docking experiments, which indicated that the 2-phenyl ring is oriented away from the binding pocket towards solvent [13]. This proposed binding mode can explain the observed tolerance towards different substituents in this position. In contrast, the insertion of an additional CH₂ group between the phenyl ring and the N2 of the pyrazol-3-one scaffold was less well tolerated, and led to a 4-fold loss in activity (**12**).

Table 2 5-CF₃ pyrazol-3-ones with different 2- and 4-substituents, and their inhibitory activity against LgtC.



Cmpd	R_2	R_3	IC_{50} (μM) ^a
6	H	3-Br, 4-OCH ₃	>50
7a	H	3-OBn	18 ± 1
7b	H	3-Br, 4-OCH ₃	3.1 ± 0.5
7c	H	H	28 ± 5
7d	H	4-Cl	25 ± 2
7e	H	2-CO ₂ CH ₂ CH ₃	>100
7f	3-CO ₂ H	3-Br, 4-OCH ₃	3.0 ± 0.3
7g	4-CO ₂ H	3-Br, 4-OCH ₃	2.9 ± 0.2
10	3-C(O)NHCH ₂ CH ₂ OH	3-Br, 4-OCH ₃	4.3 ± 0.4
12	n/a	n/a	12 ± 2

^aLgtC was pre-incubated with inhibitor (**7a**, **7c-7g**, **10**: 0.1-100 μM ; **7b**, **12**: 0.1-50 μM) or DMSO, UDP-Gal (28 μM), MnCl₂ (5 mM), CIP (10 U/mL), CEL (1 mg/mL), and Triton (0.01%) for 30 mins at 30 °C in 13 mM HEPES buffer (pH 7.0). Lactose (2 mM) was added, and the reactions were incubated for 20 mins at 30 °C. Each compound was tested in triplicate; results are presented as average ± SD.

2.2.2 Covalent inhibition kinetics for selected pyrazol-3-ones

Although IC_{50} values are commonly used as a measure of potency and for SAR studies, they are not ideal for the analysis of covalent inhibitors [18]. The interaction between a covalent inhibitor and its target can be separated into a reversible, non-covalent binding step, and an irreversible inactivation step (Fig. S1). The first step can be described quantitatively by the inhibition constant K_i , and the second step by the inactivation rate k_{inact} . Experimental protocols have been established to determine these kinetic parameters, and thus the relative contribution of each step to overall inhibition [17]. To fully understand the covalent inhibition kinetics in the

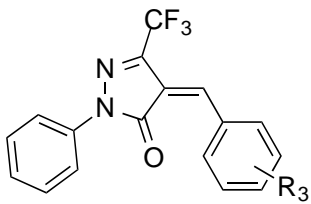
pyrazol-3-one series, we used these protocols to determine the K_i and k_{inact} values of eight selected derivatives (Fig. S2), and correlate them with IC_{50} values (Table 3).

Within this set of 5- CF_3 pyrazol-3-ones, k_{inact} values did not vary significantly ($0.9\text{-}2.5 \times 10^{-3} \text{ s}^{-1}$). This suggests that independent of the substitution pattern at the 4-benzylidene substituent, the covalent bond formation rate is of a similar order of magnitude for all eight derivatives. In contrast, a considerable spread of K_i values was observed for the same derivatives (5-150 μM). This indicates that different substituents on the 4-benzylidene moiety directly affect the reversible binding affinity of these inhibitors for LgtC. Taken together, these results suggest that it is non-covalent binding, not covalent inactivation, that drives LgtC inhibition in this series of pyrazol-3-ones. This interpretation is supported by the good correlation between K_i values and IC_{50} values (Table 3). The rank orders of K_i and IC_{50} values correspond almost perfectly, with only a single outlier (**7d**). This correlation is even stronger between IC_{50} values and the ratio of k_{inact}/K_i . Thus, inhibitors with a high k_{inact}/K_i ratio have low IC_{50} values, as previously observed for other covalent inhibitors [19].

The availability of K_i and k_{inact} values also enabled us to delineate SAR for the different substitution patterns on the 4-benzylidene moiety (Table 3). Almost all derivatives with one or more substituents on the 4-benzylidene moiety displayed higher k_{inact}/K_i values, and hence better affinity for LgtC, than the derivative **7c** bearing an unsubstituted 4-benzylidene. Regarding the effect of individual modifications, substitution of the 3-position (**7a**, **7j**) was generally less favourable than substitution of the 4-position. Most notably, moving a benzyloxy substituent from position 3 to position 4 led to a 10-fold improvement, both in terms of K_i and IC_{50} value (**7h** vs **7a**). This suggests that a large substituent in position 3 is disadvantageous for non-covalent binding affinity, which may be indicative of a

possible steric clash with the enzyme in this position. In contrast, substituents at position 4 were generally very well tolerated, with the exception of a chloro substituent (**7d**).

Table 3 Kinetic parameters for covalent inhibition of LgtC by selected 5-CF₃ pyrazol-3-ones.



Cmpd	R ₃	k_{inact} ($\times 10^{-3} \text{ s}^{-1}$) ^a	K_i (μM) ^a	k_{inact}/K_i ($\text{M}^{-1}\text{s}^{-1}$)	IC_{50} (μM) ^b
7a	3-OBn	1.8 ± 0.1	50 ± 9	36	38 ± 13
7b	3-Br, 4-OCH ₃	1.2 ± 0.07	7.1 ± 1.1	163	6.4 ± 1.6
7c	H	2.0 ± 0.2	153 ± 31	13	63 ± 8
7d	4-Cl	0.9 ± 0.1	49 ± 18	18	80 ± 26
7h	4-OBn	1.1 ± 0.07	4.7 ± 1.0	238	3.3 ± 0.6
7i	4-OCH ₃	1.5 ± 0.07	19 ± 2	80	8.9 ± 1.8
7j	3-Cl	1.6 ± 0.3	88 ± 33	18	64 ± 5
7k	4-OH	2.5 ± 0.2	6.8 ± 1.5	370	5.8 ± 0.5

^aEach compound was tested in triplicate; results are presented as average \pm SD. For details see ESI, Fig. S2. ^bLgtC was pre-incubated with inhibitor (**7a**: 0.1-100 μM ; **7b**, **7h**, **7i**, **7k**: 0.1-50 μM ; **7d**, **7j**: 0.1-200 μM ; **7c**: 0.1-250 μM) or DMSO, UDP-Gal (28 μM), MnCl₂ (5 mM), CIP (10 U/mL), CEL (1 mg/mL), and Triton (0.01%) for 20 mins at 30 °C in 13 mM HEPES buffer (pH 7.0). Lactose (2 mM) was added, and the reactions were incubated for 20 mins at 30 °C. Each compound was tested in triplicate; results are presented as average \pm SD.

2.3 Microbiological evaluation of selected inhibitors

2.3.1 Growth inhibition assay

To assess the activity of this class of LgtC inhibitors against live bacteria, we evaluated the 5-CF₃ pyrazol-3-ones **7a** and **7b** against non-typeable *H. influenzae* (NTHi) strain R2866. For direct comparison, we also included the prototype inhibitor

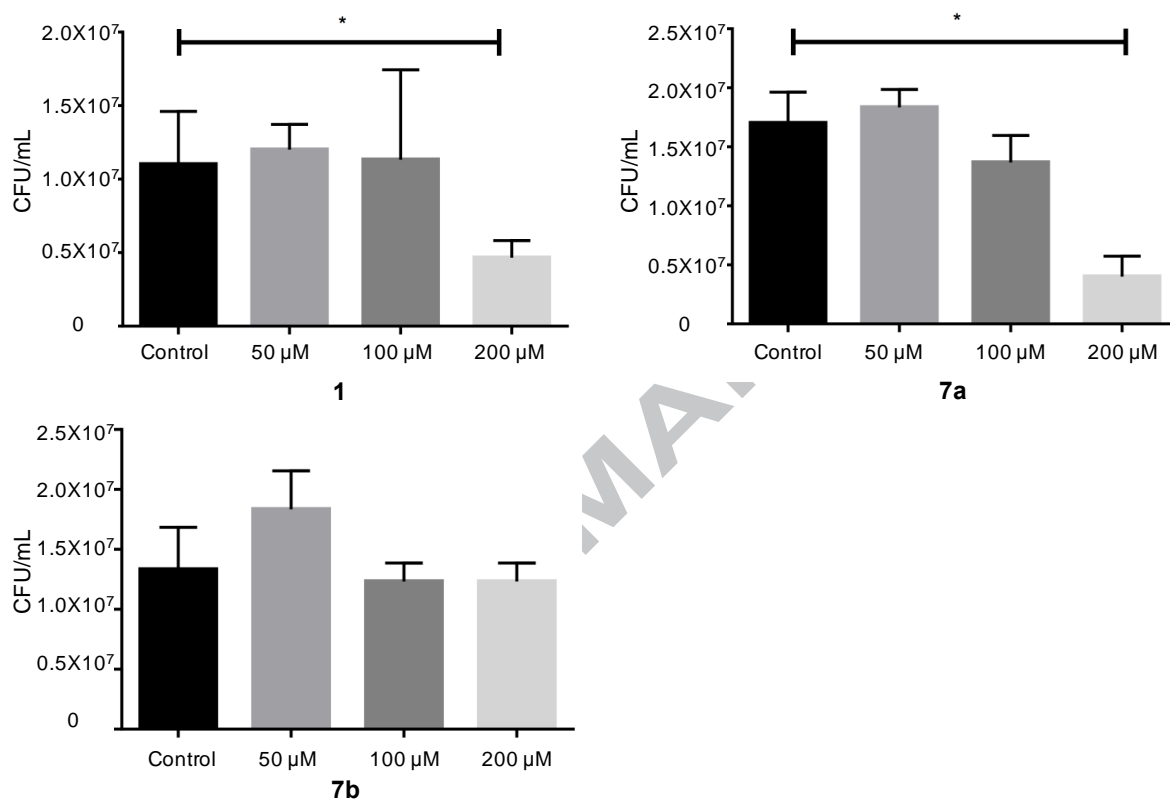
1 [13] in these experiments. NTHi strain R2866 was first isolated by Nizet from the blood of children with a meningitis infection [20]. Despite its lack of a capsular polysaccharide structure, this strain has been reported to be serum-resistant at a similar level as encapsulated type b *H. influenzae* [10]. The unusual serum resistance and increased virulence of the R2866 strain has been linked to the *lgtC* gene and the expression of terminal digalactoside epitopes on LOS structures in the outer membrane [9]. LgtC inhibitors may therefore be able to reduce this increased serum resistance and potentiate serum killing. Such a mechanism would make them useful as potential anti-virulence agents [21].

Before putting this hypothesis to the test in serum survival experiments, we first evaluated the effect of **1**, **7a** and **7b** on bacterial growth. To identify the optimal time point for growth inhibition experiments, we monitored the growth of strain R2866 by measuring the optical density (OD) over 20 hours. A single colony of the organism was grown in the supplemented Brain Heart Infusion broth (sBHI) at 37 °C for 19 hours, and the OD₅₉₀ was recorded at various time points (Fig S3). The doubling time of *H. influenzae* R2866 was 2 hours. The organism reached the stationary phase after 10-12 hours, with a maximal OD₅₉₀ of 2.6, followed by a decline in growth.

To assess the potential toxicity of pyrazol-3-ones **1**, **7a** and **7b** against R2866, we used a bacterial viable count method [22] to quantify viable bacteria after inhibitor treatment. Thus, a stationary culture of *H. influenzae* was diluted to the required OD₅₉₀ and incubated for 1 h with inhibitors at various concentrations (0-200 µM), or DMSO as the control. Samples were centrifuged, and the cell pellet was washed twice to remove excess inhibitors. Bacterial samples were serially diluted and plated on

chocolate agar plates. The cultures were incubated at 37 °C, 5% CO₂ for 24 hours, and the viable count was recorded (Fig. 3).

Fig. 3 Activity of pyrazol-3-ones **1**, **7a**, and **7b** in the *H. influenzae* R2866 growth inhibition assay.^a



^aConditions: *H. influenzae* R2866 was incubated with inhibitors **1**, **7a**, or **7b** (0-200 μM, final percentage of DMSO: 10%) at 37 °C for 1 h. Excess inhibitor was removed by centrifugation, and the cell pellet was washed with sBHI twice. Resuspended cell samples were plated on agar plates and incubated at 37 °C, 5% CO₂ for 24 h. Viable count was recorded and data were analysed with GraphPad Prism v6.0. Each concentration was tested in triplicate; results are shown as the mean. Statistical analysis was performed by an unpaired t-test; *P < 0.05.

At concentrations up to 100 μM, none of the inhibitors had a significant effect on bacterial growth under these conditions. This is not unexpected, as LgtC is not essential for bacterial viability. This lack of growth inhibitory activity is, in fact, desirable, as an anti-virulence agent is, ideally, devoid of bactericidal or bacteriostatic activity [11]. However, in cultures treated with **1** or **7a** at 200 μM we did

observe a significant reduction in bacterial growth ($P < 0.05$). This suggests that at this concentration, these pyrazol-3-ones interfere with one or more targets other than LgtC that are critical for bacterial viability.

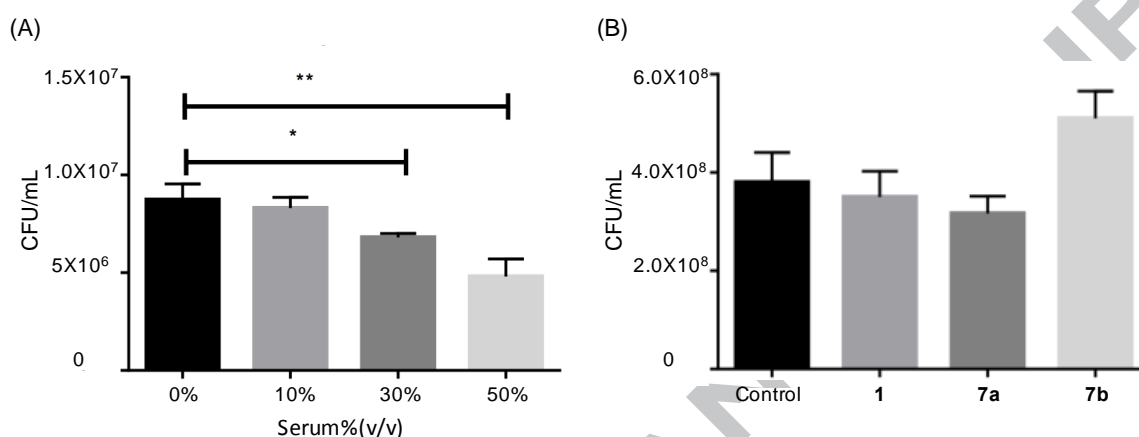
2.3.2 Serum survival assay

To test the hypothesis that LgtC inhibitors may be able to increase the sensitivity of *H. influenzae* strain R2866 to serum, we designed a serum survival experiment. First, bacteria in the stationary phase were exposed to various concentrations of normal human serum (NHS) for 1 h, before plating the cultures on agar plates. The general protocol followed that of the growth inhibition assay. As shown in Fig. 4A, 10% (v/v) NHS had no killing effect on R2866 compared to untreated bacteria. However, the viable count dropped significantly in samples treated with 30% and 50% NHS, with P values less than 0.05 (30%) and 0.01 (50%), respectively. These results showed that as expected, strain R2866 was only susceptible to serum killing at high levels of NHS.

To assess if LgtC inhibitors may enhance the killing effect of serum, we next determined bacterial viability in the presence of both serum (30% v/v) and inhibitors. As our goal was to attenuate bacterial serum resistance rather than kill the bacteria outright, we tested **1**, **7a**, and **7b** at concentrations that did not affect bacterial growth (**1** and **7a**: 100 μ M; **7b**: 50 μ M). The overnight culture of R2866 was diluted to the required OD_{590} , followed by incubation with both serum and the respective inhibitor for 1 h at 37 °C. Serum and free inhibitors were removed by centrifugation. Cell pellet was washed twice with sBHI and plated on agar plates. After 24 h incubation, the viable count was recorded (Fig. 4B). No significant reduction in serum resistance

was observed in the presence of inhibitor. This suggests that none of these three pyrazol-3-ones potentiates serum killing of *H. influenzae* strain R2866.

Fig. 4 Serum survival assay in the absence (a) or presence of inhibitors (b).^a



^aConditions: (A) *H. influenzae* R2866 was incubated with different concentrations of serum for 1 h at 37 °C, followed by centrifugation to remove excess serum. The cell pellet was plated on agar plates and incubated for another 24 h at 37 °C, 5% CO₂. Viable count was recorded, and data were analysed by GraphPad Prism v6.0. Each concentration was tested in triplicate; results are shown as the mean. Statistical analysis was performed by an unpaired t-test; *P < 0.05, **P < 0.01. (B) Bacteria were exposed to 30% NHS and inhibitor (**1**: 100 μM; **7a**: 100 μM; **7b**: 50 μM) for 1 h at 37 °C (Control: 30% NHS). Serum and inhibitors were removed by centrifugation. Cell pellet was plated on agar plates, and incubated for another 24 h at 37 °C, 5% CO₂. Viable count was recorded, and data were analysed by GraphPad Prism v6.0. Each concentration was tested in triplicate; results are shown as the mean.

3. Conclusions

We have recently identified 5-substituted pyrazol-3-ones as novel, non-substrate-like inhibitors of the bacterial glycosyltransferase LgtC with a covalent mode of action [13]. In this study, we have systematically explored the effect of different substituents in position 2, 4 and 5 of the pyrazol-3-one scaffold on inhibitory activity. We found that an electron-withdrawing CF₃ substituent in position 5 is superior not only to the electron-donating 5-CH₃ substituent of the prototype inhibitor, but also to other electron-withdrawing groups. Focusing specifically on derivatives

with a 5-CF₃ substituent, we carried out a detailed analysis of inhibition kinetics to dissect the non-covalent binding and covalent inactivation steps that are characteristic for covalent inhibitors [17]. This analysis showed that different substitution patterns at the 4-benzylidene moiety have limited influence on the reactivity of the electrophilic Michael acceptor warhead, but a strong effect on non-covalent binding. In conjunction with IC₅₀ values, these results indicate that non-covalent binding rather than covalent inactivation is the driver for overall inhibitory activity in this 5-CF₃ pyrazol-3-one series of LgtC inhibitors. Non-catalytic cysteines are a common motif in bacterial GTs [13]. The insights from this study may therefore also be useful for the rational development of covalent inhibitors against other bacterial GTs.

LgtC increases serum resistance in some *H. influenzae* strains and is therefore a potential target for anti-virulence drug discovery [10]. This prompted us to evaluate selected pyrazol-3-ones against the serum-resistant *H. influenzae* strain R2866. While none of these LgtC inhibitors affected bacterial growth at concentrations up to 100 µM, neither did they enhance serum killing. A possible explanation for this disappointing result is the phase variable expression of LgtC. Several genes related to serum resistance in *H. influenzae*, including *lgtC*, are subject to phase variation via slipped strand mispairing of DNA, a mechanism that allows bacterial pathogens to rapidly and reversibly adapt to changing environments [8, 23]. The expression of the digalactoside epitope in NTHi is controlled by tetranucleotide repeats [23] and, as a consequence of slipped strand mispairing, is turned on or off at high frequency, resulting in structural heterogeneity of the LOS structures [23]. Although *H. influenzae* strain R2866 was, as expected, remarkably resistant to NHS in our serum survival assay, under the current conditions of the assay, this serum resistance

cannot be linked directly to the presence of the digalactoside epitope, or the expression of LgtC. The phase variable expression of LgtC under the conditions of the serum survival assay therefore provides a likely explanation for the observed lack of activity of our LgtC inhibitors in this assay.

As phase variation is an important adaptation mechanism of bacterial pathogens *in-vivo*, the results from this study suggest that LgtC inhibitors have probably only limited potential as anti-virulence agents. Due to their covalent mode of action, the 5-CF₃ pyrazol-3-ones described herein are, however, attractive templates for the development of novel labeling reagents. Such labeling reagents would enable the direct labeling of LgtC and related phase-variable GTs in bacterial cells and cell lysates. Because of their minimal effect on bacterial growth, the 5-CF₃ pyrazol-3-ones described herein are ideally suited for such applications. The development of such probes is currently underway [24].

4. Experimental section

4.1 Chemistry

All chemical reagents were obtained commercially and used as received. Microwave-assisted reactions were conducted on a Monowave 300 microwave synthesis reactor from Anton Paar. Target compounds and synthetic intermediates were purified by flash chromatography column and characterised by TLC, ¹H-NMR, ¹³C-NMR, and ESI-MS. Flash chromatography columns were packed wet. Thin layer chromatography (TLC) was performed on precoated aluminium plates (Silica Gel 60 F254, Merck). Compounds were visualized by exposure to UV light (254/365 nm). NMR spectra were recorded on a Bruker BioSpin at 400 MHz (¹H) or 100 MHz (¹³C). Chemical shifts (δ) are reported in ppm, and coupling constants (J) are reported in

Hz. The order of citation in parentheses is (i) multiplicity (s, singlet; d, doublet; t, triplet; q, quartet and m, multiplet), (ii) coupling constant (J) quoted in Hertz to the nearest 0.1 Hz, (iii) number of equivalent nuclei (by integration). Mass spectra were recorded at the EPSRC National Mass Spectrometry Service Centre, Swansea. Bromine-containing compounds **6**, **7b**, **7f**, **7g**, **8a-d**, **10** and **12** contain the naturally occurring isotope mixture of the two stable bromine isotopes Br-79 and Br-81. Pyrazol-3-ones **1**, **7a**, and **7b** were synthesised as previously reported [13].

Phenyl-3-(trifluoromethyl)-1H-pyrazol-5-ol (3a). [13] Phenylhydrazine (433 mg, 4 mmol) and ethyl 4,4,4-trifluoroacetoacetate (736 mg, 4 mmol) were dissolved in glacial acetic acid. The reaction mixture was stirred at 110 °C until TLC (hexane/EtOAc 1:1) showed complete consumption of the starting material. Upon cooling a white solid precipitated from the solution and was filtered and washed with ice-cold ethanol. Purification by flash column chromatography afforded the title compound as a white solid (652 mg, 2.86 mmol, 72 %). $^1\text{H-NMR}$ (400 MHz, $\text{DMSO-}d_6$, ppm) δ : 5.94 (s, 1H), 7.39 (t, $J = 8.0$ Hz, 1H), 7.52 (t, $J = 8.0$ Hz, 2H), 7.71 (d, $J = 8.0$ Hz, 2H), 12.49 (s, 1H) ppm; $^{13}\text{C-NMR}$ (100 MHz, $\text{DMSO-}d_6$, ppm) δ : 85.6, 121.3 (q, $^1J_{\text{CF}} = 267$ Hz), 122.3, 127.2, 129.1, 137.7, 140.4 (d, $^2J_{\text{CF}} = 37$ Hz), 153.7 ppm.

Ethyl 2-(5-hydroxy-1-phenyl-1H-pyrazol-3-yl)acetate (3b) [25]. Phenylhydrazine (2.5 g, 22.8 mmol) and diethyl 3-oxopentanedioate (4.6 g, 22.8 mmol) were dissolved in EtOH, and the mixture was heated to reflux for 2 h. Upon completion, the reaction mixture was cooled down, followed by evaporation to remove most of the solvent. Purification by flash column chromatography afforded the title compound (2.3 g, 9.3 mmol, 41%) as a light yellow powder. $^1\text{H-NMR}$ (400 MHz, CDCl_3 , ppm) δ : 1.32 (t, $J =$

7.1 Hz, 3H), 3.60 (s, 2H), 3.65 (s, 2H), 4.24 (q, $J = 7.1$ Hz, 2H), 7.21 (t, $J = 7.4$ Hz, 1H), 7.35-7.46 (m, 2H), 7.83-7.88 (m, 2H).

Ethyl 5-hydroxy-1-phenyl-1H-pyrazole-3-carboxylate (3c) [25]. The title compound was obtained as a light yellow solid (6.7 g, 28.8 mmol, 61%) from phenylhydrazine (5.4 g, 50 mmol) and diethylmalonate sodium salt (10 g, 48 mmol) under the conditions described for **3b**. $^1\text{H-NMR}$ (400 MHz, $\text{DMSO-}d_6$, ppm) δ : 1.29 (t, $J = 7.1$ Hz, 3H), 4.28 (t, $J = 10.7$ Hz, 2H), 5.96 (s, 1H), 7.37 (t, $J = 7.4$ Hz, 1H), 7.51 (t, $J = 7.9$ Hz, 2H), 7.73 (d, $J = 7.5$ Hz, 2H), 12.15 (s, 1H).

5-Hydroxy-1-phenyl-1H-pyrazole-3-carboxamide (3d). **3c** (1.3 g, 5.6 mmol) was added into 28% ammonium hydroxide aqueous solution and heated to reflux for 12 h. Then the solution was neutralized with hydrochloric acid, followed by addition of cold water. Precipitate was formed and filtered. The powder residue was further purified by flash column chromatography to afford the title compound (431 mg, 2.1 mmol, 38%) as a grey powder. $^1\text{H-NMR}$ (400 MHz, $\text{DMSO-}d_6$, ppm) δ : 5.88 (s, 1H), 7.25 (s, 1H), 7.34 (t, $J = 7.4$ Hz, 1H), 7.44-7.56 (m, 3H), 7.78 (d, $J = 7.5$ Hz, 2H), 11.95 (s, 1H).

5-Hydroxy-1-phenyl-1H-pyrazole-3-carboxylic acid (3e). To a solution of **3c** (928 mg, 4 mmol) in ethanol was added 1 N aqueous NaOH solution. The mixture was stirred at room temperature for 3 h. Most of the organic solvent was evaporated, and the residue was acidified with 1 N HCl solution. Precipitate was formed and filtered to afford the title compound (745 mg, 3.6 mmol, 91%) as a white powder. $^1\text{H-NMR}$ (400

MHz, DMSO- d_6 , ppm) δ : 5.93 (s, 1H), 7.36 (t, J = 7.4 Hz, 1H), 7.43-7.56 (m, 2H), 7.73 (d, J = 7.5 Hz, 2H), 12.05 (s, 1H), 12.75 (s, 1H).

4-(5-Hydroxy-3-(trifluoromethyl)-1H-pyrazol-1-yl)benzoic acid (4a). The title compound was obtained as a white solid (1.4 g, 5.1 mmol, 61%) from 4-hydrazinylbenzoic acid (1.3 g, 8.5 mmol) and ethyl 4,4,4-trifluoroacetoacetate (1.32 mL, 8.5 mmol) under the conditions described for **3a**. $^1\text{H-NMR}$ (400 MHz, DMSO- d_6 , ppm) δ : 5.94 (s, 1H), 7.90 (d, J = 9.0 Hz, 2H), 7.99 (d, J = 9.0 Hz, 2H), 11.78 (s, 1H), 12.49 (s, 1H).

3-(5-Hydroxy-3-(trifluoromethyl)-1H-pyrazol-1-yl)benzoic acid (4b). The title compound was obtained as a white solid (1.83 g, 6.7 mmol, 75%) from 3-hydrazinylbenzoic acid (1.37 g, 9.0 mmol) and ethyl 4,4,4-trifluoroacetoacetate (1.32 mL, 9.0 mmol) under the conditions described for **3a**. $^1\text{H-NMR}$ (400 MHz, DMSO- d_6 , ppm) δ : 5.98 (s, 1H), 7.65 (t, J = 7.9 Hz, 1H), 7.91-7.96 (m, 1H), 7.98-8.04 (m, 1H), 8.30 (t, J = 1.9 Hz, 1H), 12.74 (s, 1H), 13.29 (s, 1H).

5-Methyl-2-phenyl-2,4-dihydro-3H-pyrazol-3-one (5) [26]. The title compound was obtained as a light yellow solid (343 mg, 1.97 mmol, 97%) from ethyl 3-oxobutanoate (264 mg, 2.03 mmol) and phenylhydrazine (219 mg, 2.03 mmol) under the conditions described for **3a**. $^1\text{H-NMR}$ (400 MHz, CDCl_3 , ppm) δ : 2.26 (s, 3H), 3.49 (s, 2H), 7.27-7.32 (m, 1H), 7.48-7.54 (m, 2H), 7.96-8.01 (m, 2H); $^{13}\text{C-NMR}$ (100 MHz, CDCl_3 , ppm) δ : 16.9, 43.0, 118.8, 125.0, 128.8, 138.0, 156.4, 170.0.

(*Z*)-4-(3-Bromo-4-methoxybenzylidene)-5-methyl-2-phenyl-2,4-dihydro-3H-pyrazol-3-one (**6**). **5** (174 mg, 1.0 mmol) and 3-bromo-4-methoxybenzaldehyde (322.5 mg, 1.5 mmol) were dissolved in glacial acetic acid. The reaction was heated to reflux until TLC showed complete consumption of starting material. The product was purified by flash column chromatography. The title compound was obtained as an orange solid (199 mg, 0.54 mmol, 54%). ¹H-NMR (400 MHz, DMSO-*d*₆, ppm) δ: 2.32 (s, 3H), 3.98 (s, 3H), 7.20 (t, *J* = 7.4 Hz, 1H), 7.32 (d, *J* = 8.8 Hz, 1H), 7.39-7.51 (m, 2H), 7.76 (s, 1H), 7.91 (d, *J* = 7.6 Hz, 2H), 8.56 (dd, *J* = 8.8, 2.1 Hz, 1H), 9.25 (d, *J* = 2.1 Hz, 1H). ¹³C-NMR (100 MHz, DMSO-*d*₆, ppm) δ: 13.1, 56.8, 110.7, 112.6, 118.4, 124.6, 124.9, 127.3, 128.8, 136.6, 138.0, 138.1, 146.6, 151.7, 159.2, 161.7. ESI-MS: *m/z* 371.03 (100%) [M+H]⁺; HR-MS: *m/z* 371.0386 (100%), 372.0419 (20%), 373.0364 (100%), 374.0396 (20%) [M+H]⁺, [C₁₈H₁₆BrN₂O₂]⁺ calcd for 371.0390, 372.0423, 373.0369, 374.0403.

(*Z*)-4-Benzylidene-2-phenyl-5-(trifluoromethyl)-2,4-dihydro-3H-pyrazol-3-one (**7c**) [15]. **3a** (141 mg, 0.5 mmol) and benzaldehyde (106 mg, 0.75 mmol) were placed in a microwave-proof glass tube and heated for 15 mins at 160 °C in a commercial microwave apparatus. The reaction was cooled to room temperature. The reaction product was precipitated by addition of ethyl acetate and hexane, collected by filtration, and recrystallized from hexane and ethyl acetate. The title compound was obtained as an orange solid (93 mg, 0.30 mmol, 59%). ¹H-NMR (400 MHz, CDCl₃, ppm) δ: 7.28-7.34 (m, 1H), 7.44-7.51 (m, 2H), 7.57 (t, *J* = 7.5 Hz, 2H), 7.65 (t, *J* = 7.4 Hz, 1H), 7.80 (s, 1H), 7.94 (dd, *J* = 8.7, 1.1 Hz, 2H), 8.55 (d, *J* = 7.3 Hz, 2H). ¹³C-NMR (100 MHz, CDCl₃, ppm) δ: 119.8 (q, ¹*J*_{CF} = 270 Hz), 120.0, 121.5, 126.3, 128.9, 129.0, 132.5, 134.5, 134.6, 137.5, 140.7 (q, ²*J*_{CF} = 37 Hz), 150.6, 161.1. ESI-MS:

m/z 317.1 (100%) $[M+H]^+$; HR-MS: m/z 317.0900 $[M+H]^+$, $[C_{17}H_{12}F_3N_2O]^+$ calcd for 317.0896.

(Z)-4-(4-Chlorobenzylidene)-2-phenyl-5-(trifluoromethyl)-2,4-dihydro-3H-pyrazol-3-one (**7d**) [15]. The title compound was obtained as an orange solid (35 mg, 0.1 mmol, 20%) from **3a** (114 mg, 0.5 mmol) and 4-chlorobenzaldehyde (106 mg, 0.75 mmol) under the conditions described for **7c**. 1H -NMR (400 MHz, $CDCl_3$, ppm) δ : 7.31 (t, J = 7.4 Hz, 1H), 7.45-7.51 (m, 2H), 7.54 (d, J = 8.7 Hz, 2H), 7.91 (d, J = 7.6 Hz, 2H), 7.72 (s, 1H), 8.52 (d, J = 8.6 Hz, 2H). ^{13}C -NMR (100 MHz, $CDCl_3$, ppm) δ : 119.7 (q, $^1J_{CF}$ = 270 Hz), 120.0, 121.8, 126.4, 129.0, 129.4, 130.9, 135.8, 137.3, 140.6 (d, $^2J_{CF}$ = 39 Hz), 141.3, 148.8, 161.1. ESI-MS: m/z 351.1 (100 %) $[M+H]^+$; 383.1 (95%) $[M+MeOH+H]^+$; 405.1 (55%) $[M+MeOH+Na]^+$; HR-MS: m/z 351.0506 $[M+H]^+$, $[C_{17}H_{11}ClF_3N_2O]^+$ calcd for 351.0507.

Ethyl (*Z*)-2-((5-oxo-1-phenyl-3-(trifluoromethyl)-1,5-dihydro-4H-pyrazol-4-ylidene)methyl)-benzoate (**7e**). The title compound was obtained as an orange solid (15 mg, 0.04 mmol, 15%) from **3a** (54 mg, 0.25 mmol) and ethyl 2-formylbenzoate (66.8 mg, 0.38 mmol) under the conditions described for **7c**. 1H -NMR (400 MHz, $CDCl_3$, ppm) δ : 1.42 (t, J = 7.1 Hz, 3H), 4.42 (q, J = 7.1 Hz, 2H), 7.25 (d, J = 7.4 Hz, 1H), 7.43 (t, J = 8.0 Hz, 2H), 7.60-7.69 (m, 2H), 7.86 (d, J = 7.7 Hz, 2H), 8.04 (d, J = 7.1 Hz, 1H), 8.19 (d, J = 7.5 Hz, 1H), 8.62 (s, 1H). ^{13}C -NMR (100 MHz, $CDCl_3$, ppm) δ : 14.2, 61.9, 119.6, 119.7 (q, $^1J_{CF}$ = 270 Hz), 121.2, 126.2, 129.0, 129.9, 131.0, 131.2, 131.7, 132.0, 132.9, 137.3, 140.5 (d, $^2J_{CF}$ = 37 Hz), 151.5, 160.9, 166.1. ESI-MS: m/z 389.1 (85%) $[M+H]^+$, 421.1 (100%) $[M+MeOH+H]^+$, 443.1 (56%) $[M+MeOH+Na]^+$; HR-MS: m/z 389.1110 $[M+H]^+$, $[C_{20}H_{16}F_3N_2O_3]^+$ calcd for 389.1108.

(*Z*)-3-(4-(3-Bromo-4-methoxybenzylidene)-5-oxo-3-(trifluoromethyl)-4,5-dihydro-1H-pyrazol-1-yl)benzoic acid (**7f**). The title compound was obtained as an orange solid (118 mg, 0.25 mmol, 50%) from **4b** (114 mg, 0.5 mmol) and 3-bromo-4-methoxybenzaldehyde (161 mg, 0.75 mmol) under the conditions described for **7c**. ¹H-NMR (400 MHz, DMSO-*d*₆, ppm) δ: 4.03 (s, 3H), 7.39 (d, *J* = 8.9 Hz, 1H), 7.65 (t, *J* = 8.0 Hz, 1H), 7.88 (d, *J* = 7.9 Hz, 1H), 7.94 (s, 1H), 8.10 (d, *J* = 8.1 Hz, 1H), 8.44 (t, *J* = 1.8 Hz, 1H), 8.71 (dd, *J* = 8.9, 2.1 Hz, 1H), 9.31 (d, *J* = 2.1 Hz, 1H), 13.19 (s, 1H). ESI-MS: *m/z* 468.98 (5%) [M+H]⁺, 499.01 (100%) [M+MeOH+H]⁺; HR-MS: *m/z* 467.0015 (100%), 467.9850 (30%), 468.9824 (50%), 469.9879 (5%) [M-H]⁻, [C₁₉H₁₁BrF₃N₂O₄]⁻ calcd for 466.9860, 467.9891, 468.9840, 469.9872.

(*Z*)-4-(4-(3-Bromo-4-methoxybenzylidene)-5-oxo-3-(trifluoromethyl)-4,5-dihydro-1H-pyrazol-1-yl)benzoic acid (**7g**) [27]. The title compound was obtained as an orange solid (66 mg, 0.14 mmol, 28%) from **4a** (114 mg, 0.5 mmol) and 3-bromo-4-methoxybenzaldehyde (161 mg, 0.75 mmol) under the conditions described for **7c**. ¹H-NMR (400 MHz, DMSO-*d*₆, ppm) δ: 4.02 (s, 3H), 7.35 (d, *J* = 8.9 Hz, 1H), 7.90 (s, 1H), 8.00 (d, *J* = 8.9 Hz, 2H), 8.06 (d, *J* = 8.9 Hz, 2H), 8.64 (d, *J* = 8.9 Hz, 1H), 9.28 (s, 1H). ESI-MS: *m/z* 467.0 (100 %) [M-H]⁻; HR-MS: *m/z* 466.9854 (100%), 467.9889 (15%), 468.9833 (100%), 469.9867 (15%) [M-H]⁻, [C₁₉H₁₁BrF₃N₂O₄]⁻ calcd for 466.9860, 467.9893, 468.9839, 469.9873.

(*Z*)-4-(4-(Benzyloxy)benzylidene)-2-phenyl-5-(trifluoromethyl)-2,4-dihydro-3H-pyrazol-3-one (**7h**). The title compound was obtained as an orange solid (31 mg, 0.07 mmol, 30%) from **3a** (57 mg, 0.25 mmol) and 4-(benzyloxy)benzaldehyde (64

mg, 0.3 mmol) under the conditions described for **7c**. $^1\text{H-NMR}$ (400 MHz, $\text{DMSO-}d_6$, ppm) δ : 5.31 (s, 2H), 7.27 (d, $J = 9.0$ Hz, 2H), 7.33 (t, $J = 7.4$ Hz, 1H), 7.38 (d, $J = 7.1$ Hz, 1H), 7.43 (t, $J = 7.2$ Hz, 2H), 7.51 (t, $J = 7.7$ Hz, 4H), 7.84 (d, $J = 7.8$ Hz, 2H), 7.91 (s, 1H), 8.81 (d, $J = 9.0$ Hz, 2H). $^{13}\text{C-NMR}$ (100 MHz, $\text{DMSO-}d_6$, ppm) δ : 70.0, 115.4, 117.56, 119.8 (q, $^1J_{\text{CF}} = 270$ Hz), 120.0, 125.9, 126.2, 128.0, 128.2, 128.5, 129.0, 136.0, 137.3, 138.2, 139.9 (d, $^2J_{\text{CF}} = 36$ Hz), 150.0, 161.1, 164.3. ESI-MS: m/z 423.1 (100 %) $[\text{M}+\text{H}]^+$; HR-MS: m/z 423.1312 $[\text{M}+\text{H}]^+$, $[\text{C}_{24}\text{H}_{18}\text{F}_3\text{N}_2\text{O}_2]^+$ calcd for 423.1315.

(*Z*)-4-(4-Methoxybenzylidene)-2-phenyl-5-(trifluoromethyl)-2,4-dihydro-3H-pyrazol-3-one (**7i**) [28]. The title compound was obtained as an orange solid (68 mg, 0.20 mmol, 39%) from **3a** (114 mg, 0.5 mmol) and 4-methoxybenzaldehyde (102 mg, 0.75 mmol) under the conditions described for **7c**. $^1\text{H-NMR}$ (400 MHz, CDCl_3 , ppm) δ : 3.96 (s, 3H), 7.06 (d, $J = 9.0$ Hz, 2H), 7.29 (t, $J = 7.4$ Hz, 1H), 7.44-7.51 (m, 2H), 7.72 (s, 1H), 7.95 (dd, $J = 8.7, 1.1$ Hz, 2H), 8.67 (d, $J = 9.0$ Hz, 2H). $^{13}\text{C-NMR}$ (100 MHz, CDCl_3 , ppm) δ : 55.82, 114.65, 118.50, 119.9 (q, $^1J_{\text{CF}} = 270$ Hz), 120.04, 126.11, 126.14, 128.96, 137.73, 138.05, 140.9 (d, $^2J_{\text{CF}} = 36$ Hz), 150.05, 161.65, 165.25. ESI-MS: m/z 347.1 (100 %) $[\text{M}+\text{H}]^+$; 379.1 (10%) $[\text{M}+\text{MeOH}+\text{H}]^+$; 401.1 (20%) $[\text{M}+\text{MeOH}+\text{Na}]^+$; HR-MS: m/z 347.1002 $[\text{M}+\text{H}]^+$, $[\text{C}_{18}\text{H}_{14}\text{F}_3\text{N}_2\text{O}_2]^+$ calcd for 347.1002.

(*Z*)-4-(3-Chlorobenzylidene)-2-phenyl-5-(trifluoromethyl)-2,4-dihydro-3H-pyrazol-3-one (**7j**) [28]. The title compound was obtained as an orange solid (74 mg, 0.21 mmol, 42%) from **3a** (114 mg, 0.5 mmol) and 3-chlorobenzaldehyde (105 mg, 0.75 mmol) under the conditions described for **7c**. $^1\text{H-NMR}$ (400 MHz, CDCl_3 , ppm) δ : 7.31 (t, $J = 7.4$ Hz, 1H), 7.49 (m, 3H), 7.58-7.64 (m, 1H), 7.70 (s, 1H), 7.91 (d, $J =$

8.6 Hz, 2H), 8.38 (d, $J = 7.8$ Hz, 1H), 8.61 (t, $J = 1.8$ Hz, 1H). ^{13}C -NMR (100 MHz, CDCl_3 , ppm) δ : 119.7 (q, $^1J_{\text{CF}} = 270$ Hz), 120.0, 122.7, 126.5, 129.1, 130.1, 132.4, 133.6, 133.8, 134.1, 135.0, 137.3, 140.4 (d, $^2J_{\text{CF}} = 36$ Hz), 148.5, 160.8. ESI-MS: m/z 351.1 (80 %) $[\text{M}+\text{H}]^+$; 383.1 (100%) $[\text{M}+\text{MeOH}+\text{H}]^+$; 405.1 (45%) $[\text{M}+\text{MeOH}+\text{Na}]^+$; HR-MS: m/z 351.0506 $[\text{M}+\text{H}]^+$, $[\text{C}_{17}\text{H}_{11}\text{ClF}_3\text{N}_2\text{O}]^+$ calcd for 351.0507.

(*Z*)-4-(4-Hydroxybenzylidene)-2-phenyl-5-(trifluoromethyl)-2,4-dihydro-3H-pyrazol-3-one (**7k**). The title compound was obtained as an orange solid (60 mg, 0.18 mmol, 35%) from **3a** (114 mg, 0.5 mmol) and 4-hydroxybenzaldehyde (92 mg, 0.75 mmol) under the conditions described for **7c**. ^1H -NMR (400 MHz, $\text{DMSO}-d_6$, ppm) δ : 6.99 (d, $J = 8.9$ Hz, 2H), 7.31 (t, $J = 7.4$ Hz, 1H), 7.42-7.55 (m, 2H), 7.79-7.89 (m, 3H), 8.74 (d, $J = 8.9$ Hz, 2H), 11.34 (s, 1H). ^{13}C -NMR (100 MHz, $\text{DMSO}-d_6$, ppm) δ : 116.10, 116.27, 119.87, 119.9 (q, $^1J_{\text{CF}} = 270$ Hz), 124.56, 126.07, 128.98, 137.40, 138.95, 140.0 (d, $^2J_{\text{CF}} = 36$ Hz), 150.34, 161.18, 165.08. ESI-MS: m/z 333.1 (100 %) $[\text{M}+\text{H}]^+$; 355.1 (20%) $[\text{M}+\text{Na}]^+$; 387.1 (25%) $[\text{M}+\text{MeOH}+\text{Na}]^+$; HR-MS: m/z 333.0847 $[\text{M}+\text{H}]^+$, $[\text{C}_{17}\text{H}_{12}\text{F}_3\text{N}_2\text{O}_2]^+$ calcd for 333.0845.

Ethyl (*Z*)-4-(3-bromo-4-methoxybenzylidene)-5-oxo-1-phenyl-4,5-dihydro-1H-pyrazole-3-carboxylate (**8a**). The title compound was obtained as an orange solid (109 mg, 0.26 mmol, 51%) from **3c** (116 mg, 0.5 mmol) and 3-bromo-4-methoxybenzaldehyde (161 mg, 0.75 mmol) under the conditions described for **7c**. ^1H -NMR (400 MHz, CDCl_3 , ppm) δ : 1.49 (t, $J = 7.1$ Hz, 3H), 4.03 (s, 3H), 4.50 (q, $J = 7.1$ Hz, 2H), 7.03 (d, $J = 8.8$ Hz, 1H), 7.30 (t, $J = 7.4$ Hz, 1H), 7.44-7.50 (m, 2H), 7.94 (d, $J = 7.5$ Hz, 2H), 8.65 (s, 1H), 8.69 (dd, $J = 8.8, 2.2$ Hz, 1H), 8.91 (d, $J = 2.2$ Hz,

1H). ^{13}C -NMR (100 MHz, CDCl_3 , ppm) δ : 14.3, 56.7, 61.9, 111.5, 112.0, 120.8, 122.1, 126.4, 127.7, 128.9, 136.6, 137.6, 139.9, 140.1, 151.2, 160.4, 161.2, 162.1. ESI-MS: m/z 429.0 (100%) $[\text{M}+\text{H}]^+$, 451.0 (25%) $[\text{M}+\text{Na}]^+$, 483.0 (35%) $[\text{M}+\text{MeOH}+\text{Na}]^+$; HR-MS: m/z 429.0444 (100%), 430.0478 (20%), 431.0423 (100%), 432.0456 (20%) $[\text{M}+\text{H}]^+$, $[\text{C}_{20}\text{H}_{18}\text{BrN}_2\text{O}_4]^+$ calcd for 429.0444, 430.0478, 431.0424, 432.0458.

Ethyl (Z)-2-(4-(3-bromo-4-methoxybenzylidene)-5-oxo-1-phenyl-4,5-dihydro-1H-pyrazol-3-yl)acetate (8b). The title compound was obtained as an orange solid (93 mg, 0.21 mmol, 53%) from **3b** (123 mg, 0.5 mmol) and 3-bromo-4-methoxybenzaldehyde (161 mg, 0.75 mmol) under the conditions described for **7c**. ^1H -NMR (400 MHz, CDCl_3 , ppm) δ : 1.31 (t, $J = 7.1$ Hz, 3H), 3.78 (s, 2H), 4.03 (s, 3H), 4.25 (q, $J = 7.1$ Hz, 2H), 7.03 (d, $J = 9.3$ Hz, 1H), 7.23 (t, $J = 7.4$ Hz, 1H), 7.38 (s, 1H), 7.44 (t, $J = 8.0$ Hz, 2H), 7.97 (d, $J = 8.5$ Hz, 2H), 8.72-8.77 (m, 2H). ^{13}C -NMR (100 MHz, CDCl_3 , ppm) δ : 14.2, 34.6, 56.6, 61.8, 111.5, 111.9, 119.4, 124.9, 125.2, 127.3, 128.8, 135.6, 138.2, 139.3, 146.1, 147.2, 159.9, 162.0, 168.8. ESI-MS: m/z 443.1 (100%) $[\text{M}+\text{H}]^+$, 475.1 (45%) $[\text{M}+\text{Na}]^+$, 479.1 (15%) $[\text{M}+\text{MeOH}+\text{Na}]^+$; HR-MS: m/z 443.0598 (100%), 444.0633 (20%), 445.0576 (100%), 446.0610 (20%) $[\text{M}+\text{H}]^+$, $[\text{C}_{21}\text{H}_{20}\text{BrN}_2\text{O}_4]^+$ calcd for 443.0601, 444.0633, 445.0581, 446.0614.

(Z)-4-(3-Bromo-4-methoxybenzylidene)-5-oxo-1-phenyl-4,5-dihydro-1H-pyrazole-3-carboxylic acid (8c). The title compound was obtained as an orange solid (160 mg, 0.40 mmol, 80%) from **3f** (103 mg, 0.5 mmol) and 3-bromo-4-methoxybenzaldehyde (161 mg, 0.75 mmol) under the conditions described for **7c**. ^1H -NMR (400 MHz, $\text{DMSO}-d_6$, ppm) δ : 3.99 (s, 3H), 7.31 (t, $J = 8.0$ Hz, 2H), 7.50 (t, $J = 8.0$ Hz, 2H), 7.87 (d, $J = 7.6$ Hz, 2H), 8.39 (dd, $J = 8.9, 2.1$ Hz, 1H), 8.57 (s, 1H), 9.25 (d, $J = 2.1$ Hz,

1H), 13.79 (s, 1H). ¹³C-NMR (100 MHz, DMSO-*d*₆, ppm) δ: 57.0, 110.9, 112.6, 119.9, 121.8, 126.0, 127.1, 129.0, 137.5, 137.6, 138.1, 141.1, 150.5, 159.9, 161.7, 162.0. ESI-MS: *m/z* 401.0 (100%) [M+H]⁺; HR-MS: *m/z* 401.0132 (100%), 402.0166 (20%), 403.0110 (100%), 404.0144 (20%) [M+H]⁺, [C₁₈H₁₄BrN₂O₄]⁺ calcd for 401.0131, 402.0165, 403.0111, 404.0145.

(*Z*)-4-(3-Bromo-4-methoxybenzylidene)-5-oxo-1-phenyl-4,5-dihydro-1H-pyrazole-3-carboxamide (**8d**). The title compound was obtained as an orange solid (60 mg, 0.15 mmol, 30%) from **3d** (102 mg, 0.5 mmol) and 3-bromo-4-methoxybenzaldehyde (161 mg, 0.75 mmol) under the conditions described for **7c**. ¹H-NMR (400 MHz, DMSO-*d*₆, ppm) δ: 4.01 (s, 3H), 7.27-7.35 (m, 2H), 7.46-7.53 (m, 2H), 7.77 (s, 1H), 8.01 (d, *J* = 7.6 Hz, 2H), 8.17 (s, 1H), 8.38 (dd, *J* = 8.9, 2.1 Hz, 1H), 8.74 (s, 1H), 9.31 (d, *J* = 2.1 Hz, 1H). ¹³C-NMR (100 MHz, DMSO-*d*₆, ppm) δ: 57.0, 110.9, 112.7, 119.5, 122.0, 125.6, 127.2, 128.9, 137.6, 137.7, 138.0, 142.8, 151.0, 159.8, 161.8, 162.6. ESI-MS: *m/z* 400.0 (100%) [M+H]⁺; HR-MS: *m/z* 400.0293 (100%), 401.0326 (20%), 402.0273 (100%), 403.0306 (20%) [M+H]⁺, [C₁₈H₁₅BrN₃O₃]⁺ calcd for 400.0291, 401.0325, 402.0271, 403.0305.

3-(5-Hydroxy-3-(trifluoromethyl)-1H-pyrazol-1-yl)-N-(2-hydroxyethyl)benzamide (**9**).

To a solution of **4b** (272 mg, 1 mmol) in DMF, HBTU (758 mg, 2.0 mmol), DIEA (387 mg, 3.0 mmol), and 2-aminoethan-1-ol (92 mg, 1.5 mmol) were added. The reaction mixture was stirred at rt for 16 h. Most of the DMF was then evaporated. The residue was diluted with water and extracted with ethyl acetate for 3 times. The combined organic layer was dried over Na₂SO₄. The crude product was purified by flash chromatograph to afford the title compound (235 mg, 0.76 mmol, 75%). ¹H-NMR

(400 MHz, DMSO- d_6 , ppm) δ : 2.79-3.01 (m, 2H), 3.52 (t, $J = 5.7$ Hz, 2H), 4.76 (s, 1H), 5.96 (s, 1H), 7.60 (t, $J = 7.9$, 1H), 7.85 (s, 1H), 8.18 (s, 1H), 8.62 (t, $J = 5.5$ Hz, 1H), 12.75 (s, 1H).

(*Z*)-3-(4-(3-Bromo-4-methoxybenzylidene)-5-oxo-3-(trifluoromethyl)-4,5-dihydro-1H-pyrazol-1-yl)-*N*-(2-hydroxyethyl)benzamide (**10**). The title compound was obtained as an orange solid (20 mg, 0.04 mmol, 9%) from **9** (126 mg, 0.4 mmol) and 3-bromo-4-methoxybenzaldehyde (129 mg, 0.6 mmol) under the conditions described for **7c**.

$^1\text{H-NMR}$ (400 MHz, DMSO- d_6 , ppm) δ : 3.52 (q, $J = 5.6$ Hz, 2H), 4.04 (s, 3H), 4.16 (t, $J = 5.7$ Hz, 2H), 7.39 (d, $J = 8.9$ Hz, 1H), 7.62 (t, $J = 7.9$ Hz, 1H), 7.79 (d, $J = 9.1$ Hz, 1H), 7.95 (s, 1H), 7.99-8.05 (m, 1H), 8.29 (s, 1H), 8.70 (dd, $J = 8.9, 2.1$ Hz, 1H), 8.77 (t, $J = 5.5$ Hz, 1H), 9.34 (d, $J = 2.1$ Hz, 1H). ESI-MS: m/z 512.04 (100%) $[\text{M}+\text{H}]^+$; HR-MS m/z 512.0422 (100%), 513.0464 (23%), 514.0415 (100%), 515.0444 (23%) $[\text{M}+\text{H}]^+$, $[\text{C}_{21}\text{H}_{18}\text{BrF}_3\text{N}_3\text{O}_4]^+$ calcd for 512.0427, 513.0455, 514.0409, 515.0435.

1-Benzyl-3-(trifluoromethyl)-1H-pyrazol-5-ol (**11**). The title compound was obtained as a light yellow solid (120 mg, 0.50 mmol, 17%) from ethyl 4,4,4-trifluoro-3-oxobutanoate (662 mg, 3.6 mmol) and benzylhydrazine (585 mg, 3 mmol) under the conditions described for **3a**. $^1\text{H-NMR}$ (400 MHz, CDCl_3 , ppm) δ : 5.08 (s, 2H), 5.59 (s, 1H), 7.10-7.26 (m, 5H), 11.07 (s, 1H).

(*Z*)-2-Benzyl-4-(3-bromo-4-methoxybenzylidene)-5-(trifluoromethyl)-2,4-dihydro-3H-pyrazol-3-one (**12**). The title compound was obtained as an orange solid (50 mg, 0.11 mmol, 28%) from **11** (97 mg, 0.4 mmol) and 3-bromo-4-methoxybenzaldehyde (103 mg, 0.48 mmol) under the conditions described for **7c**. $^1\text{H-NMR}$ (400 MHz,

CDCl₃, ppm) δ : 4.04 (s, 3H), 5.05 (s, 2H), 7.03 (d, $J = 8.8$ Hz, 1H), 7.35-7.40 (m, 5H), 7.55 (s, 1H), 8.68 (dd, $J = 8.8, 2.2$ Hz, 1H), 8.88 (d, $J = 2.2$ Hz, 1H). ¹³C-NMR (100 MHz, CDCl₃, ppm) δ : 48.9, 56.7, 111.6, 112.2, 119.5, 119.8 (q, $^1J_{CF} = 270$ Hz), 127.2, 128.0, 128.3, 128.8, 136.0, 136.4, 139.5 (d, $^2J_{CF} = 36$ Hz), 139.7, 147.8, 160.7, 162.4. ESI-MS: m/z 439.03 (100 %) [M+H]⁺, 471.05 (50%) [M+MeOH+H]⁺, 493.03 (65%) [M+MeOH+Na]⁺; HR-MS: m/z 439.0262 (100%), 440.0297 (20%), 441.0241 (92%), 442.0275 (20%) [M+H]⁺, [C₁₉H₁₅BrF₃N₂O₂]⁺ calcd for 439.0264, 440.0295, 441.0243, 442.0276.

4.2 Biochemistry

4.2.1 Inhibition assays

Recombinant LgtC from *Neisseria meningitidis* was expressed and purified as previously described [13]. For single concentration experiments and IC₅₀ experiments, LgtC activity was adjusted to 20-50% turnover of UDP-Gal donor. Recombinant LgtC was activated with DTT (10 mM, in HEPES buffer) in a 1:1 ratio for 30 mins at 30 °C prior to each experiment. Inhibition experiments were carried out with pre-incubation of LgtC with inhibitor, in the presence of donor, as previously described [13]. Briefly, aliquots (15 μ L each) of activated LgtC, MnCl₂ (5 mM), CEL (1 mg/mL), CIP (10 U/mL), Triton (0.01%) and HEPES buffer (13 mM, pH 7.0) were combined with inhibitor at various concentrations in DMSO (15 μ L, 10% final DMSO concentration) or DMSO only (15 μ L, control) in the requisite microplate wells. UDP-Gal donor (15 μ L, 28 μ M) was added, and the mixtures were pre-incubated for the requisite time at 30 °C. Lactose acceptor (30 μ L, 2 mM) or HEPES buffer (30 μ L, control) were added, and the reactions were incubated for 20 mins at 30 °C. Reactions were stopped by addition of Malachite Green Reagent A (30 μ L). The

microplate was shaken carefully, and Malachite Green Reagent B (30 μ L) was added. The colour was allowed to develop over 20 mins, and the absorbance in each well was recorded at 620 nm on a Polarstar Optima plate reader (BMG Labtech). The absorbance measurements were used to calculate enzyme activity.

4.2.2 Determination of kinetic parameters k_{inact} and K_i .

K_i and k_{inact} values were determined as previously described [13]. LgtC activity was determined at various concentrations of inhibitor (**7a**, **7d**, **7j**: 0-200 μ M; **7b**, **7i**: 0-50 μ M; **7c**: 0-250 μ M; **7h**: 0-100 μ M) and after different pre-incubation times (0, 5, 10, and 20 mins). Enzyme activity is expressed as percentage of control (DMSO only) and plotted on a semi-logarithmic scale over pre-incubation time. From these plots, values for K_{obs} were extracted by exponential regression using the equation $enzyme\ activity\ [\%] = A \times e^{-K_{obs} \times t}$, where t = pre-incubation time. Observed rate constants K_{obs} were extracted from the plots, re-plotted over inhibitor concentrations, and fitted to the hyperbolic equation $K_{obs} = k_{inact} \times [I]/(K_i + [I])$. All experiments were performed in triplicate.

4.3 Microbiology

4.3.1 Bacterial growth assay

H. influenzae R2866 was streaked out on a bacitracin chocolate agar plate (chocolate agar: Columbia blood agar with 10% lysed horse blood) and incubated at 37 °C, 5% CO₂ overnight. A single colony was chosen from the plate and inoculated into 10 mL sBHI broth (supplemented Brain Heart Infusion broth: 7.5 g Brain Heart Infusion in 200 mL deionised water, 10 μ m/mL NAD, and 10 μ L/mL Hemin), followed by incubation at 37 °C, 180 rpm overnight. 200 μ L of the overnight culture was added

into fresh sBHI and incubated at 37 °C 180 rpm. OD₅₉₀ was recorded at various time points. The data were tested in triplicate and presented as average. The number of viable count: OD₅₉₀ 0.7 was approximately 4*10⁸ CFU/mL.

4.3.2 Growth inhibition assays

A single colony of *H. influenzae* R2866 was chosen from the agar plate and inoculated into 10 mL sBHI broth, followed by incubation at 37 °C 180 rpm overnight. The overnight culture was diluted to OD₅₉₀ 0.7 with sBHI. 900 µL of the bacterial culture was incubated with 100 µL of the respective inhibitor stock solution in DMSO (**1**: 0.5 mM; **7a**: 1 mM; **7b**: 2 mM) at 37 °C for 1 h. Upon completion, excess inhibitor was removed by centrifugation, and the cell pellet was washed with sBHI twice. Cells were re-suspended in sBHI and serially diluted. Finally, 10 µL of the diluted samples were plated on chocolate agar plates and incubated for another 24 h at 37 °C, 5% CO₂. Viable count was recorded and data were analysed by GraphPad Prism v6.0. Each inhibitor concentration was tested in triplicate; results are presented as the mean. Statistical analysis was performed by an unpaired t-test; *P < 0.05.

4.3.3 Serum survival assay

A single colony of *H. influenzae* R2866 was chosen from the agar plate and inoculated into 10 mL sBHI broth, followed by incubation at 37 °C, 180 rpm overnight. The overnight culture was diluted to OD₅₉₀ 0.7 with sBHI. Bacteria were exposed for 1 h at 37 °C either to human serum alone (0-50%, v/v), or to human serum (30%, v/v) and inhibitor (**1** and **7a**: 100 µM; **7b**: 50 µM). Serum and excess inhibitors were removed by centrifugation, and the cell pellet was washed twice with sBHI. Cells were re-suspended in sBHI and serially diluted. 10 µL of the diluted samples were

plated on chocolate agar plates and incubated for another 24 h at 37 °C, 5% CO₂.

Viable count was recorded and data were analysed by GraphPad Prism v6.0. Each experiment was carried out in triplicate; results are presented as the mean.

Statistical analysis was performed by an unpaired t-test; *P < 0.05, **P < 0.01.

ACCEPTED MANUSCRIPT

Acknowledgement

This study was supported by a King's China Award (to Y.X.). We thank the EPSRC National Mass Spectrometry Facility (Swansea) for the recording of mass spectra, and Camille Metier for recording the NOESY spectrum of compound **6**.

ACCEPTED MANUSCRIPT

Supplementary data

Supplementary data associated with this article can be found, in the online version,
at <http://dx.doi.org/xxx>

ACCEPTED MANUSCRIPT

References

- [1] (a) Lu, Q.; Li, S.; Shao, F., Sweet talk: protein glycosylation in bacterial interaction with the host. *Trends Microbiol.* **2015**, *23*, 630-641; (b) Tytgat, H.L.; Lebeer, S., The sweet tooth of bacteria: common themes in bacterial glycoconjugates. *Microbiol. Mol. Biol. Rev.* **2014**, *78*, 372-417.
- [2] Gloster, T.M. Advances in understanding glycosyltransferases from a structural perspective. *Curr. Opin. Struct. Biol.* **2014**, *28*, 131-141.
- [3] Davies, G.J.; Gloster, T.M.; Henrissat, B. Recent structural insights into the expanding world of carbohydrate-active enzymes. *Curr. Opin. Struct. Biol.* **2005**, *15*, 637-645.
- [4] Sánchez-Rodríguez, A.; Tytgat, H.L.; Winderickx, J.; Vanderleyden, J.; Lebeer, S.; Marchal, K. A network-based approach to identify substrate classes of bacterial glycosyltransferases. *BMC Genomics.* **2014**, *15*, 349.
- [5] Helm, J.S.; Hu, Y.; Chen, L.; Gross, B.; Walker, S. Identification of active-site inhibitors of MurG using a generalizable, high-throughput glycosyltransferase screen. *J. Am. Chem. Soc.* **2003**, *125*, 11168-11169.
- [6] Persson, K.; Ly, H.D.; Dieckelmann, M.; Wakarchuk, W.W.; Withers, S.G.; Strynadka, N.C.J. Crystal structure of the retaining galactosyltransferase LgtC from *Neisseria meningitidis* in complex with donor and acceptor sugar analogs. *Nat. Struct. Biol.* **2001**, *8*, 166-175.
- [7] Lombard, V.; Golaconda, R.H.; Drula, E.; Coutinho, P.M.; Henrissat, B. The carbohydrate-active enzymes database (CAZy) in 2013. *Nucleic Acids Res.* **2014**, *42*, D490-495.

- [8] Clark, S.E.; Eichelberger, K.R.; Weiser, J.N. Evasion of killing by human antibody and complement through multiple variations in the surface oligosaccharide of *Haemophilus influenzae*. *Mol. Microbiol.* **2013**, *88*, 603-618.
- [9] Griffin, R.; Bayliss, C.D.; Herbert, M.A.; Cox, A.D.; Makepeace, K.; Richards, J.C.; Hood, D.W.; Moxon, E.R. Digalactoside expression in the lipopolysaccharide of *Haemophilus influenzae* and its role in intravascular survival. *Infect. Immun.* **2005**, *73*, 7022-7026.
- [10] Erwin, A.L.; Allen, S.; Ho, D.K.; Bonthius, P.J.; Jarisch, J.; Nelson, K.L.; Tsao, D.L.; Unrath, W.C.T.; Watson, M.E.; Gibson, B.W.; Apicella, M.A.; Smith, A.L. Role of *LgtC* in resistance of nontypeable *Haemophilus influenzae* strain R2866 to human serum. *Infect. Immun.* **2006**, *74*, 6226-6235.
- [11] Allen, R.C.; Popat, R.; Diggle, S.P.; Brown, S.P. Targeting virulence: can we make evolution-proof drugs? *Nat. Rev. Microbiol.* **2014**, *12*, 300-308.
- [12] Descroix, K.; Pesnot, T.; Yoshimura, Y.; Gehrke, S.; Wakarchuk, W.; Palcic, M.M.; Wagner, G.K. Inhibition of galactosyltransferases by a novel class of donor analogues. *J. Med. Chem.* **2012**, *55*, 2015-2024.
- [13] Xu, Y.; Smith, R.; Vivoli, M.; Ema, M.; Goos, N.; Gehrke, S.; Harmer, N.J.; Wagner, G.K. Covalent inhibitors of *LgtC*: a blueprint for the discovery of non-substrate-like inhibitors for bacterial glycosyltransferases. *Bioorg. Med. Chem.* **2017**, *25*, 3182-3194.
- [14] Tietze, L.F.; Brumby, T.; Pretor, M.; Remberg, G. Intramolecular Hetero-Diels-Alder Reaction of Alkylidene- and Benzylidenepyrazolones and Benzylideneisoxazolones. Investigations toward the Conformation of the Transition State. *J. Org. Chem.* **1988**, *53*, 810-820.

- [15] Zhang, J.; Yang, S.; Zhang, K.; Chen, J.; Deng, H.; Shao, M.; Zhang, H.; Cao, W., An efficient and highly stereoselective synthesis of novel trifluoromethylated *trans*-dihydrofuro[2,3-*c*]pyrazoles using arsonium ylides. *Tetrahedron* **2012**, *68*, 2121-2127.
- [16] Tedaldi, L.; Evitt, A.; Göös, N.; Jiang, J.; Wagner, G.K. A practical glycosyltransferase assay for the identification of new inhibitor chemotypes. *MedChemComm.* **2014**, *5*, 1193-1201.
- [17] Singh, J.; Petter, R.C.; Baillie, T.A.; Whitty, A. The resurgence of covalent drugs. *Nat. Rev. Drug Discovery.* **2011**, *10*, 307-317.
- [18] (a) Klutchko, S. R.; Zhou, H.; Winters, R. T.; Tran, T. P.; Bridges, A. J.; Althaus, I. W.; Amato, D. M.; Elliott, W. L.; Ellis, P. A.; Meade, M. A., Tyrosine kinase inhibitors. 19. 6-Alkynamides of 4-anilinoquinazolines and 4-anilinopyrido [3,4-*d*] pyrimidines as irreversible inhibitors of the erbB family of tyrosine kinase receptors. *J. Med. Chem.* **2006**, *49*, 1475-1485; (b) Zapf, C. W.; Gerstenberger, B. S.; Xing, L.; Limburg, D. C.; Anderson, D. R.; Caspers, N.; Han, S.; Aulabaugh, A.; Kurumbail, R.; Shakya, S., Covalent inhibitors of interleukin-2 inducible T cell kinase (itk) with nanomolar potency in a whole-blood assay. *J. Med. Chem.* **2012**, *55*, 10047-10063; (c) Kwarcinski, F. E.; Fox, C. C.; Steffey, M. E.; Soellner, M. B., Irreversible inhibitors of c-Src kinase that target a nonconserved cysteine. *ACS Chem. Biol.* **2012**, *7*, 1910-1917.
- [19] (a) Dounay, A. B.; Anderson, M.; Bechle, B. M.; Campbell, B. M.; Claffey, M. M.; Evdokimov, A.; Evrard, E.; Fonseca, K. R.; Gan, X.; Ghosh, S., Discovery of brain-penetrant, irreversible kynurenine aminotransferase II inhibitors for schizophrenia. *ACS Med. Chem. Lett.* **2012**, *3*, 187-192; (b) Wu, L.; Jiang, J.; Jin, Y.; Kallemeijn, W. W.; Kuo, C.-L.; Artola, M.; Dai, W.; van Elk, C.; van Eijk, M.; van der

Marel, G. A., Activity-based probes for functional interrogation of retaining β -glucuronidases. *Nat. Chem. Biol.* **2017**, *13*, 867-873.

[20] Nizet, V.; Colina, K.F.; Almquist, J.R.; Rubens, C.E.; Smith, A.L. A virulent nonencapsulated *Haemophilus influenzae*. *J. Infect. Dis.* **1996**, *173*, 180-186.

[21] Clatworthy, A.E.; Pierson, E.; Hung, D.T. Targeting virulence: a new paradigm for antimicrobial therapy. *Nat. Chem. Biol.* **2007**, *3*, 541-548.

[22] Kogure, K.; Simidu, U.; Taga, N., A tentative direct microscopic method for counting living marine bacteria. *Can. J. Microbiol.* **1979**, *25*, 415-420.

[23] Weiser, J.N.; Love, J.M.; Moxon, E.R., The molecular mechanism of phase variation of *H. influenzae* lipopolysaccharide. *Cell* **1989**, *59*, 657-665.

[24] Xu, Y.; Uddin, N.; Wagner, G.K. Covalent Probes for Carbohydrate-Active Enzymes: From Glycosidases to Glycosyltransferases. *Methods Enzymol.* **2018**, *598*, 237-265.

[25] Bianchini, R.; Bonanni, M.; Corsi, M.; Infantino, A. S., Viable and straightforward approach to the preparation of water soluble pyrazol-5-one derivatives through glycoconjugation. *Tetrahedron* **2012**, *68*, 8636-8644.

[26] Ma, R.; Zhu, J.; Liu, J.; Chen, L.; Shen, X.; Jiang, H.; Li, J., Microwave-assisted one-pot synthesis of pyrazolone derivatives under solvent-free conditions. *Molecules* **2010**, *15*, 3593-3601.

[27] Schepetkin, I. A.; Khlebnikov, A. I.; Kirpotina, L. N.; Quinn, M. T. Novel Small-Molecule Inhibitors of Anthrax Lethal Factor Identified by High-Throughput Screening. *J. Med. Chem.* **2006**, *49*, 5232-5244.

[28] Sobahi, T. R., Thermal condensation of 3-trifluoromethyl- / and 3-amino-1-phenyl-2-pyrazolin-5-ones with aromatic aldehydes. Synthesis of 4-arylidene-

pyrazolones and pyrazolopyranopyrazoles. *Indian J. Chem., Sect. B: Org. Chem.*

Incl. Med. Chem. **2006**, *45B(5)*, 1315-1318.

ACCEPTED MANUSCRIPT

Author contributions

GW, BW and JC designed the study; YX synthesised and characterised the inhibitors, and carried out the biochemical experiments; YX and TM carried out the microbiological assays, with support from JC and CD; GW and YX wrote the manuscript; all authors commented on the manuscript.

Conflict of interest

The authors declare no conflict of interest.

ACCEPTED MANUSCRIPT